Study of CZTSSe based solar cells with different ETMs by SCAPS

Lhoussayne Et-taya
LM3ER-OTEA Department of physics,
Faculty of Sciences and Techniques
Moulay Ismail University of Meknes
Errachidia, Morocco
l.ettaya@edu.umi.ac.ma

Touria Ouslimane
LM3ER-OTEA Department of physics,
Faculty of Sciences and Techniques
Moulay Ismail University of Meknes
Errachidia, Morocco
ouslimanetouria@gmail.com

Abdellah Benami
LM3ER-OTEA Department of physics,
Faculty of Sciences and Techniques
Moulay Ismail University of Meknes
Errachidia, Morocco
a.benami@fste.umi.ac.ma
https://orcid.org/0000-0001-5516-5660

Abstract

Third-generation thin-film solar cells based on CZTSSe are highly promising because of their excellent optoelectrical properties, earth-abundant, and non-toxicity of its constituent elements. In this work, the performance of CZTSSe based solar cells with TiO2, CdS, and ZnSe as electron transporting materials (ETMs) was numerically investigated using the Solar Cell capacitance Simulator (SCAPS). The effect of the active layer's thickness and electron affinity, different buffer layers and the contour plot of the operating temperature versus thickness of the CdS buffer layer were studied. The results show that the optimum power conversion efficiency for CdS, TiO2 and ZnSe, as the ETMs, is 23.16%, 23.13%, and 22.42%, respectively.

Keywords: CZTSSe, Third-generation thin-film, SCAPS, efficiency, ETMs.

I. INTRODUCTION

Photovoltaic cells are used to convert large amounts of sunlight to electricity directly. Many studies have recently been conducted to improve the efficiency of thin-film solar cells (TFSCs). Because of their extraordinary properties, TFSCs based on CZTSSe and related materials have attracted increased interest as an absorber layer in third-generation photovoltaic devices. CZTSSe is a p-type conductivity semiconductor with a tunable direct bandgap of 0.95-1.5 eV, a large absorption coefficient of over $10^4 cm^{-1}$, a low cost (earth-abundant), and non-toxic element composition [1]. The certified power conversion efficiency (PCE) of CZTSSe was reported to be up to 12.62%, which is lower than that of CIGS and CdTe (23.4% and 22.1%, respectively). It should be improved for large-scale photovoltaic applications to overcome the scarcity of In, Ge, and Te, as well as the toxicity of Cd [2-5].

There has been lots of research into replacing toxic ETM (CdS) with alternative materials in CZTSSe-based TFSCs. As a result, we propose and simulated three device structures with buffer layers of CdS, TiO_2, and ZnSe using SCAPS-1D software. The effect of several parameters on device performance (V_{oc}, J_{sc}, FF, and PCE) was investigated, including thickness, electron affinity, various buffer layers, and temperature.

II. Methodology

The schematic cross-section of the TFSC structure used in this study is shown in Fig. 1. The device under investigation consists of a Mo back contact that serves as the positive terminal, the p-CZTSSe active layer in which electron-hole pairs are generated after absorption of incident photons. Following that, CdS, TiO2, or ZnSe ETM was used to align the absorber and the window layer. The buffer layer is then stacked with i-ZnO, which is capped by a ZnO: Al window layer that acts as a transparent conductive oxide (TCO) to collect charges.

SCAPS is a program developed at the University of Gents in Belgium [6]. It is widely used for the simulation of various types of TFSCs. The SCAPS simulation results have been reported to agree well with the corresponding experimental results, which provides a convincing reason to use them in this study [4]. The software is based on solving the fundamental semiconductor equations ((1), (2), and (3)), namely the Poisson equation and the hole and electron continuity equations. It computes the band diagram in a steady-state, the recombination profile, and carrier transport in one dimension. The equations are shown below [4,7,8].

$$\frac{\partial^2 \Psi}{\partial x^2} + \frac{q}{\varepsilon}\left[p(x) - n(x) + N_D - N_A + \rho_p - \rho_n\right] = 0 \qquad \textbf{(1)}$$

$$\frac{1}{q}\frac{dJ_p}{dx} = G_{op}(x) - R(x) \qquad \textbf{(2)}$$

$$\frac{1}{q}\frac{dJ_n}{dx} = -G_{op}(x) + R(x) \qquad \textbf{(3)}$$

Here q is the electron's charge, ε is the dielectric constant, Ψ is the electrostatic potential and, N_A (N_D) is the density of acceptor-like (donor-like). p (n), ρ_p (ρ_n), and J_p (J_n) are hole (electron) concentration, hole (electron) density, electron distribution, and hole (electron) current density, respectively. R is the net recombination from direct and indirect recombination, and G_{op} is the optical generation rate.

The values of the device and material parameters used in this study are taken from the literature, experimental, theory, and reasonable estimation [7,8,10] and are summarized in Table 1.

The device was illuminated with an AM 1.5 spectrum with a light power of 1000 W/m^2. This study's shunt and series resistances were 600 Ω/cm^2 and 1.5 Ω/cm^2, respectively [4].

IEECP'21, July 29-30, 2021, Silicon Valley, San Francisco, CA – USA

DOI : ***https://dx.doi.org/10.6084/10.6084/m9.figshare.14546610***

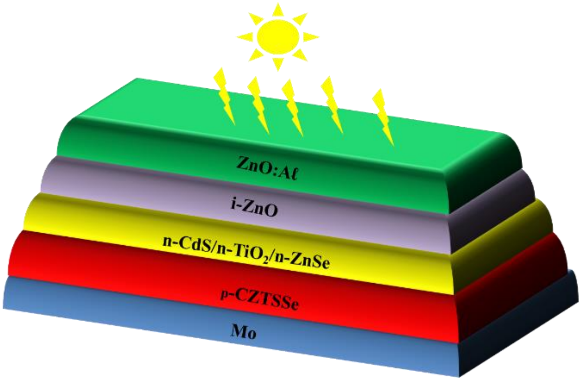

Fig.1. Structure of CZTSSe cell

Table.1 Parameters used in the simulation [7,8,10]

Parameters	ZnO:Al	i-Zno	n-TiO_2	n-ZnSe	n-CdS	p-CZTSSe
d (nm)	200	50	50	50	Variable	Variable
E_g(eV)	3.3	3.3	3.26	2.90	2.4	Variable
χ (eV)	4.4	4.4	4.2	4.02	4.2	Variable
ε (eV)	9	9	10	10	10	13.6
N_c (cm^{-3})	2.2x10^{18}	2.2x10^{18}	2.2x10^{18}	2.2x10^{18}	2.2x10^{18}	2.2x10^{18}
N_v (cm^{-3})	1.8x10^{19}	1.8x10^{19}	1.8x10^{19}	1.8x10^{19}	1.8x10^{19}	1.8X10^{19}
V_{th} e^- (cm/s)	10^7	10^7	10^7	10^7	10^7	10^7
V_{th} p (cm/s)	10^7	10^7	10^7	10^7	10^7	10^7
μ_n(cm^2/Vs)	10^2	10^2	10^2	25	10^2	10^2
μ_h (cm^2/Vs)	25	25	25	100	25	25
N_D (cm^{-3})	10^{20}	10^{19}	10^{18}	10^{18}	10^{17}	0
N_A (cm^{-3})	0	10^{19}	0	0	0	10^{18}
α (cm^{-1})	[4]	[4]	[10]	[10]	[4]	[4]

d: Thickness, Eg: Bandgap, χ: Electron Affinity, ε: Dielectric permittivity, Nc: Density of states in CB, Nv: Density of states in VB, Vth e^-: Thermal velocity of electron, Vth p: Thermal velocity of hole, μn: Electron mobility, μh: Hole mobility, N_D: Donor density, N_A: Acceptor density, α: Absorption coefficient

III. Results and discussion

A. Effect of the CZTSSe absorber layer's thickness

The absorber layer is crucial in enhancing device efficiency. In this context, simulations with CdS, TiO_2, and Znse buffer layers were used to examine the solar cell's performance in terms of the CZTSSe absorber layer. The thickness of the CZTSSe the absorber layer varied from 500 nm to 3000 nm, with a fixed ETM thickness of 50 nm. As the thickness of the CZTSSe absorber layer increases, more photons are absorbed, resulting in more electron-hole pairs [10]. Fig.2. depicts the variation of photovoltaic parameters (V_{oc}, J_{sc}, FF, PCE) as a function of CZTSSe absorber layer thickness, in which the result is in good agreement with Beer-Lamberts law. Table 2 summarizes the changes in all device parameters caused by various ETMs for absorber thicknesses of 500 nm and 3000 nm.

Table. 2 The effect of the ETM layer on the photovoltaic parameters for absorber thicknesses of 500 nm and 3000 nm.

Buffer layer	CZTSSe thickness (nm)	Voc (V)	Jsc(mA/cm^2)	FF (%)	PCE (%)
CdS	500	0,6708	29,55026	74,78	14,82
	3000	0,7245	42,6436	74,96	23,16
TiO_2	500	0,6706	29,37618	74,7	14,72
	3000	0,7245	42,6101	74,93	23,13
ZnSe	500	0,6703	29,45534	70,24	13,87
	3000	0,7243	42,58405	72,68	22,42

B. Effect of the electron affinity of the absorber layer

Figure 3 depicts the effect of absorber layer CZTSSe electron affinity on photovoltaic cell performance. The electron affinity of the absorber layer varied from 4,35 eV (CZTSe) to 4,5eV (CZTS) as extracted from the reference [4]. We can see that VOC, FF, and PCE values increase until a maximum value of χ=4,41eV is reached, then decrease with further increase of χ. On the other hand, Jsc decreases linearly with the electron affinity. Because increasing the absorber layer's electron affinity reduces the number of photons reaching the absorbing layer, the amount of current generated, and the short circuit current decreases.

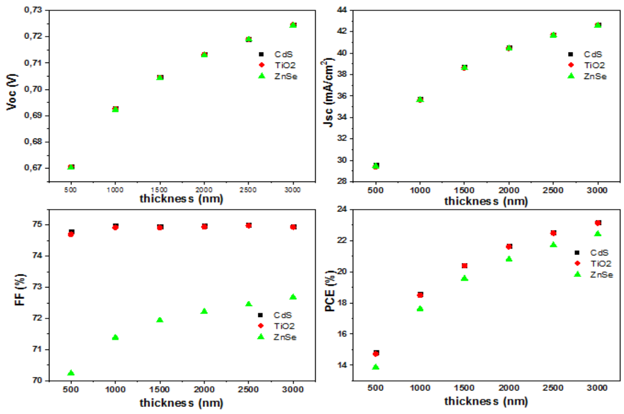

Fig.2. Effect of various thickness of CZTSSe absorber layer with the different buffer layers

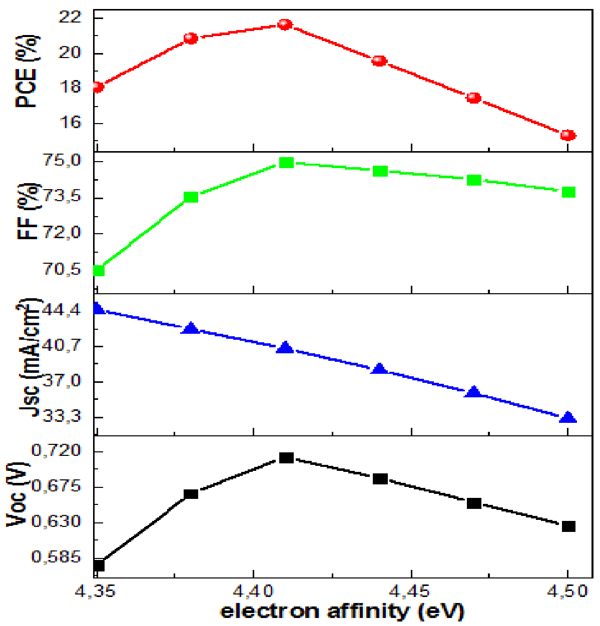

Fig.3. Variation of PCE, FF, Jsc, and Voc as a function of CZTSSe electron affinity

C. Impact of the CdS buffer layer thickness and Temperature contour plot

The buffer layer and operating temperature are well known to affect the performance of solar cells. As a consequence, the CdS buffer layer thickness and operating temperature have been increased to improve performance, from 30 nm to 70 nm and from 240 °C to 320°C, respectively. As shown in Fig. 4, the all-output parameters are not affected by the thickness of CdS. On the other hand, the increase in temperature induces a decrease in PCE, FF, and V_{oc}; this decrease was significant from the ambient temperature of 300°C. However, J_{sc} rises as the temperature rises.

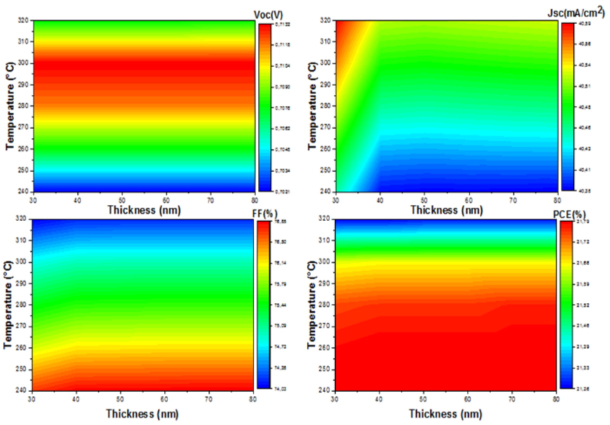

Fig.4: Contour plot of solar cell output as a function of the CdS buffer layer thickness and operating temperature.

IV. Conclusion

In this paper, numerical simulations of CZTSSe-based TFSCs were performed using the SCAPS-1D software. Three different solar cells with buffer layers of CdS, TiO_2, and ZnSe were investigated in order to find a safe alternative to the toxic CdS. Maximum PCE of CZTSSe solar cells with CdS, TiO2, and ZnSe buffer layers was predicted to be 23.16%, 23.13%, and 22.42% at ambient temperature and 3000 nm active layer, respectively. As a result, TiO_2 may be a viable choice for producing and manufacturing low-cost, high-efficiency Cd-free CZTSSe heterojunction solar cells.

V. ACKNOWLEDGMENTS

The authors are very much grateful to Dr Burgelman for providing SCAPS-1D software.

VI. REFERENCES

[1] G. Altamura, J. Vidal, Chem. Mater. 28 (2016) 3540–3563.
[2] S. Enayati Maklavani, S. Mohammadnejad, Opt. Quantum Electron. 52 (2020)
[3] G.K. Gupta, A. Dixit, Opt. Mater. (Amst). 82 (2018) 11–20
[4] L. Et-taya, T. Ouslimane, A. Benami, Sol. Energy 201 (2020) 827–835
[5] A.E. Benzetta, M. Abderrezek, M.E. Djeghlal, J. Nano- Electron. Phys. 10 (2018) 6–10
[6] M. Burgelman, K. Decock, S. Khelifi, A. Abass, Thin Solid Films 535 (2013) 296–301
[7] A. Benami, J. Energy Power Eng. 13 (2019) 32–36
[8] T. Ouslimane, L. Et-taya, L. Elmaimouni, A. Benami, Heliyon 7 (2021) e06379
[9] M. Atowar Rahman, Sol. Energy 215 (2021) 64–76
[10] H. Fujiwara, R.W. Collins, Spectroscopic Ellipsometry for Photovoltaics, 2018
[11] F.A. Jhuma, M.Z. Shaily, M.J. Rashid, Mater. Renew. Sustain. Energy 8 (2019) 1–7
[12] N. Cheng, W. Li, S. Sun, Z. Zhao, Z. Xiao, Z. Sun, W. Zi, L. Fang, Mater. Sci. Semicond. Process. 90 (2019) 59–64